Alias-Free Digital Click Modulator

Leandro Stefanazzi, Alejandro R. Oliva, and Eduardo E. Paolini

***Abstract*—An alias-free, discrete-time click modulator is developed in this paper. Previous approaches rely on translating the continuous-time click modulator to a discrete-time setting, although a key component in the click modulator—the analytic exponential modulator-cannot be exactly transformed to the discrete domain. Every discrete-time version of the click modulator reported in the literature is prone to aliasing effects that are ameliorated, but not eliminated, using interpolation techniques.**

The precision of the switching times of the output square wave is critical to click modulation because uncertainties in their determination adversely affect the performance and SNR of the modulator. A novel method that uses frequency domain information to compute these switching times without error is also presented.

This two techniques are used to develop an off-line discrete-time click modulator that achieves a SNR larger than 180 dB for both multitonal and bandpass signals.

***Index Terms*—Click modulation, digital modulation, power amplifiers, power conversion, pulse width modulation, switching converters.**

I. Introduction

PULSE-WIDTH MODULATION (PWM) is one of the most widely used modulation technique for power conversion over the years due to the low complexity of the analog modulator. Nowadays the industry is replacing analog PWM modulators by their digital counterpart. Nevertheless, the discrete-time implementation of PWM (also known as *uniform PWM* or UPWM) has a major drawback: the appeareance of baseband distortion composed by a combination of derivatives of the modulating signal, together with carrier harmonics phase-modulated by the input signal and its temporal derivatives [1], that is impossible to remove using linear filtering. Many solutions have been proposed to ameliorate this problem [2]–[18]. Interpolation and noise shaping [8], [12], sigma-delta modulation [6] and practical solutions for the finite resolution of the duty cycle [10], [11], [13], [14], [16] have been explored. In [2] the binary wave is filtered to control the harmonic level of the synthesized PWM signal and in [3] dynamic (time-varying) FIR filtering is applied prior to interpolation. In [4], nonlinearities are compensated with a neural network trained using the model of the digital modulator and [9] presents a method for recursively computing NPWM using UPWM output. A completely different approach is used in [19]–[22], where the sinusoidal signal is generated using bit-stream representation and digital logic hardware. Alternative digital modulation methods are also found in the literature, such as nonsinusoidal carrier-based/space vector PWM [23], constant on/off-time modulation for DC/DC converters [24] or feedforward delta modulation [25]. Other authors deal with minimization of switching losses [26], [27] and dead-time compensation of digital PWM modulators [28]. Digital feedback of the power stage's output is used in [5] and [7], which allows the linearization of the overall system. Even if nonlinearities are reduced, many of these solutions rely on specialized hardware, such as [17] where a 12-bit oversampling A/D converter and a delta-sigma modulator are integrated in a chip aimed at motor drive applications, or [15] where an all-digital implementation, with proprietary digital sigma-delta modulator is discussed. However, none of the previous techniques completely removes distortion components from the baseband.

Click modulation [29] is a phase modulation that encodes the modulating signal into the switching times of a square wave. Originally conceived as an analog modulation, the generated signal has its baseband separated from the high frequency components by a guard band; therefore, the information can be recovered with no distortion with a low-pass filter (LPF). The guard band allows a lower switching frequency than that required by traditional PWM-based schemes, increasing the efficiency of the switching stage. The main drawback of click modulation is its algorithmic complexity, that complicates hardware [30] and even off-line software [31] implementations, and has postponed its widespread use.

In spite of this, the first harwdare implementations of click modulation were reported in 1999 [30], [32]–[34]. Three DSPs applying 24 bits fixed-point arithmetic with a total power of 233 MMACs per second, as well as 8-times digital oversampling filter were used to implement the system for a reduced bandwidth. Additionally, two FPGAs acted as a digital pulse former featuring 10-bits time resolution to position the edges of the square wave. In [35] a complete audio band implementation is described using five DSPs and augmenting the FPGAs' clock frequency. Lately [36], an analog-to-digital converter was introduced to sample the input signal and feed a single DSP processor capable of running in real time the complete click modulation algorithm. Similarly to [35] the pulse former was implemented with an FPGA. An off-line software implementation of a discrete-time click modulator was presented in [31] that is suitable for applications such as portable audio and signal generation.

Manuscript received November 30, 2011; revised March 14, 2012 and May 24, 2012; accepted June 11, 2012. Date of publication October 02, 2012; date of current version January 09, 2013. This work was supported in part by PGI UNS 24/ZK21, ANPCyT PAE-PICT-2007-02344, PIP-CONICET 02671, and PIP-CONICET 0617. Paper no. TII-11-881.

L. Stefanazzi and A. Oliva are with the Consejo Nacional de Investigaciones Científicas y Técnicas (CONICET), Buenos Aires 8000, Argentina (e-mail: lstefanazzi@uns.edu.ar).

E. Paolini is with the Comisión de Investigaciones Científicas (CIC), CP: 1900, La Plata, Buenos Aires, Argentina. He is also with Instituto de Inv. en Ingeniería Eléctrica Alfredo Desages IIIE (UNS-CONICET), Departamento de Ingeniería Eléctrica y de Computadoras. Universidad Nacional del Sur, Buenos Aires 8000, Argentina.

Color versions of one or more of the figures in this paper are available online at http://ieeexplore.ieee.org.

Digital Object Identifier 10.1109/TII.2012.2221470

The idea relies on generating the switching times of the square wave using encoding software running on a PC that implements the modulator [37]. The square wave is then regenerated using a commercial DSP that features a high resolution PWM module and recovered with a LPF.

All the previous implementations [30]–[36] derive the discrete-time click modulator by following the continuous-time scheme developed in [29] and replacing every continuous-time signal processing stage by a discrete-time counterpart. Although some of them can be easily translated, a key component of the click modulator, referred to as the *analytic exponential modulator* (AEM) cannot be deployed as a discrete-time exact equivalent because of frequency-domain aliasing. Although reasonable performance can be obtained by interpolation and using higher switching rates, these solutions reduce the advantages of click modulation.

In this article a novel discrete-time version of a click modulator is presented. It is based entirely in discrete-time signals and transforms properties, and it is an exact equivalent of [29] but in a discrete-time setting. This approach significantly reduces the amount of processing required in previous works. In addition, an alternative method for zero-crossing computation is introduced. It is demonstrated that using frequency information it is possible to compute the exact time instants at which the underlying continuous-time signal crosses the time axis. The combination of these two techniques allows the exact implementation of the discrete-time click modulator using non-oversampled discrete-time inputs.

This article is organized as follows. Continuous-time click modulation is reviewed in Section II. Section III details the proposed discrete-time click modulator. An off-line implementation of the discrete-time click modulator is tested and the results are summarized in Section IV, where a comparison between click modulation and PWM is also performed. Finally, conclusions and future work are discussed in the last section.

II. Continuous-Time Click Modulator

Click modulation [29] is based on analytic modulation theory [38] and angle modulation [39], [40]. It is a phase modulation that produces binary signals with the property that the intermodulation products appear above a user defined frequency. This allows recovering the input information with zero distortion using a simple LPF. Further details can be found in [29], [41]–[45].

The block diagram of a continuous-time click modulator is shown in Fig. 1. The input is a real bandpass signal $x(t)$ whose spectrum $X(f)$ is comprised within $[-f_H, -f_L] \cup [f_L, f_H]$. If $\hat{x}(t)$ is the Hilbert transform of $x(t)$ the analytic signal $x_A(t)$ is defined as $x_A(t) = x(t) + j\hat{x}(t)$. The spectrum $X_A(f)$ is not zero only in the interval $[f_L, f_H]$ of the positive frequency axis.

The analytic signal $x_A(t)$ is phase-modulated by the AEM. The spectrum $Z(f)$ of its output $z(t) = e^{-jx_A(t)}$ extends over the entire positive frequency axis. The frequency content above a user-defined frequency f_U is removed by the $H_H(f)$ LPF. Its output $z_f(t)$ is shifted and reversed in frequency producing the real signal $s(t)$

$$s(t) = \mathrm{Re}\left\{\overline{z_f}(t)e^{j2\pi f_c t}\right\}$$

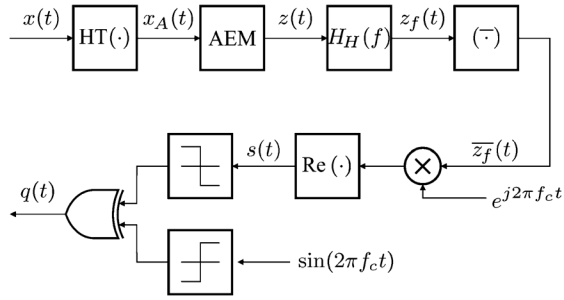

Fig. 1. Continuous-time click modulator.

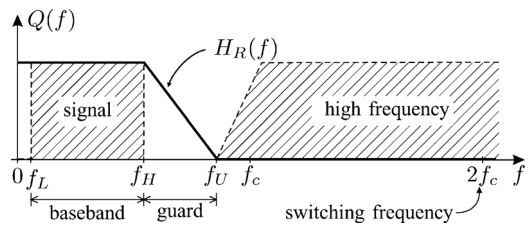

Fig. 2. Spectrum of the click-modulated signal.

where f_c is the frequency of a sinusoidal carrier $x_c(t) = \sin(2\pi f_c t)$. The binary output signal $q(t)$ is derived from both the zeros of $s(t)$ and the zeros of the carrier $x_c(t)$: $q(t)$ transitions from "low" to "high" ("high" to "low") each time the carrier $x_c(t)$ (the signal $s(t)$) crosses the real axis. Because the transitions corresponding to the zeros of the carrier occur at half its period, the switching frequency of $q(t)$ is twice the carrier frequency f_c only if the zeros of $s(t)$ lay in between the zeros of the carrier. This imposes an upper limit for the amplitude of the input signal $x(t)$ [29]. The typical spectrum of a click-modulated signal $q(t)$ is shown in Fig. 2. Due to the action of the LPF $H_H(f)$, the frequency range comprised between f_H and the (ideal) filter corner frequency f_U has no spectral content, and therefore acts as a guard band between the frequency range of the signal $x_A(t)$ and the harmonic content generated by the modulation process. The signal content can be recovered without distortion using another LPF with frequency response $H_R(f)$ as depicted in Fig. 2.

The pair AEM-LPF is the core of click modulation. The AEM takes an analytic signal $x_A(t)$ as input and generates the output signal $z(t) = e^{-jx_A(t)}$. The frequency behaviour of the AEM can be analyzed by expressing the exponential function as a power series,

$$\begin{aligned} z(t) &= e^{-jx_A(t)} \\ &= \sum_{\ell=0}^{\infty} \frac{1}{\ell!}\left[-jx_A(t)\right]^{\ell} \\ &= 1 + z_1(t) + \frac{1}{2!}z_2(t) + \frac{1}{3!}z_3(t) + \cdots \end{aligned}$$

with $z_\ell(t) = [-jx_A(t)]^\ell$, and $z_0(t) = 1$. Note that the module of the spectrum $Z_\ell(f)$ of $z_\ell(t)$ coincides with the module of the spectrum of $x_A^\ell(t)$, i.e., $|Z_\ell(f)| = |\mathcal{F}\{[-jx_A(t)]^\ell\}|$. The spectrum $Z(f)$ of $z(t)$ is given by

$$Z(f) = \sum_{\ell=0}^{\infty} \frac{1}{\ell!} Z_\ell(f), \tag{1}$$

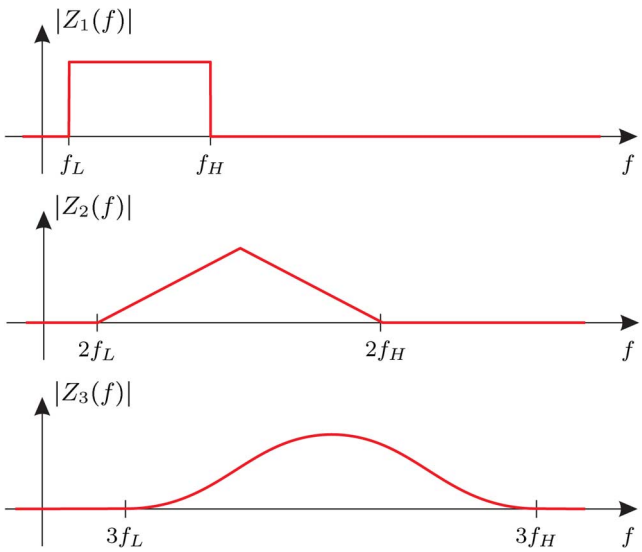

Fig. 3. Spectrum of the signals $z_1(t)$, $z_2(t)$ and $z_3(t)$.

where $Z_\ell(f)$ is the Fourier transform of $z_\ell(t) = [-jx_A(t)]^\ell$, and $Z_0(f) = \delta(f)$. The spectrum $Z_\ell(f)$ can be computed using the modulation theorem of the Fourier transform [46], that states that multiplication in time domain represents convolution in the frequency domain. Therefore,

$$\begin{aligned} Z_\ell(f) &= Z_1(f) * \cdots * Z_1(f) \\ &= Z_{\ell-1}(f) * Z_1(f) \end{aligned}$$

that can be computed as the frequency convolution between $Z_{\ell-1}(f)$ and $Z_1(f)$:

$$Z_\ell(f) = \begin{cases} \int_\theta^\psi Z_{\ell-1}(\nu) Z_1(f-\nu)d\nu, & \text{if } \ell f_L \leqslant f \leqslant \ell f_H \\ 0, & \text{otherwise.} \end{cases} \tag{2}$$

The integration interval is $[\theta, \psi]$, where $\theta = \max\{(\ell-1)f_L, f - f_H\}$ and $\psi = \min\{(\ell-1)f_H, f - f_L\}$. This expression reveals that if the spectrum $Z_1(f)$ of $z_1(t) = -jx_A(t)$ vanishes outside the band $[f_L, f_H]$, in general the spectrum $Z_\ell(f)$ of $z_\ell(t) = [-jx_A(t)]^\ell$ is not identically zero within the band $[\ell f_L, \ell f_H]$. In other words, the spectrum of increasing-order terms $z_\ell(t)$ extends over larger frequency bands. As an example, Fig. 3 shows the module of $Z_1(f)$, $Z_2(f)$, and $Z_3(f)$, which are the spectra of $z_1(t) = -jx_A(t)$, $z_2(t) = [-jx_A(t)]^2$ and $z_3(t) = [-jx_A(t)]^3$, respectively, assuming that $z_1(t)$ is an analytic, bandlimited signal with spectrum $Z_1(f) = u(f - f_L) - u(f - f_H)$.

According to (1), the computation of $Z(f)$ involves adding infinite terms $Z_\ell(f)$, each of an increasing bandwidth, and therefore $Z(f)$ is defined over the entire positive frequency axis with infinite spectral extension. However, the analytic LPF with frequency response

$$H_H(f) = \begin{cases} 1, & \text{if } 0 < f < f_U \\ 0, & \text{otherwise} \end{cases} \tag{3}$$

bandlimits the output of the AEM, and therefore, the following stages that involve spectral inversion and frequency shifting result in no distortion in the baseband.

The spectrum $Z_f(f)$ of the output $z_f(t)$ of the filter can be written as

$$\begin{aligned} Z_f(f) &= Z(f)H_H(f) \\ &= \left(\sum_{\ell=0}^{\infty} \frac{1}{\ell!} Z_\ell(f)\right) H_H(f) \\ &= \sum_{\ell=0}^{\infty} \frac{1}{\ell!} Z_\ell(f) H_H(f). \end{aligned} \tag{4}$$

Although the ℓ-th term $Z_\ell(f)$ extends over the frequency interval $[\ell f_L, \ell f_H]$, the corresponding term $Z_\ell(f)H_H(f)$ in (4) only occupies the band $[\ell f_L, f_U]$. Therefore, the only contributing terms in (4) are those for which $\ell f_L < f_U$; i.e., (4) can be replaced by a *finite* summation

$$Z_f(f) = \sum_{\ell=0}^{L_f} \frac{1}{\ell!} Z_\ell(f) H_H(f) \tag{5}$$

where $L_f = \lceil f_U / f_L \rceil$ and $\lceil x \rceil$ the ceil function, i.e., the smallest integer not smaller than x. Each term in (5) occupies the frequency band $[\ell f_L, f_U]$, and can be computed using (2) for $f \in [\ell f_L, \min\{\ell f_H, f_U\}]$. This equation is the continuous-time version of the ideally filtered AEM output and will be referred to as CT-AEMF.

The filter of (3) is crucial in assuring that click modulation preserves the baseband of the analytic modulating signal $x_A(t)$. It can be proved that if this filter is removed, the block diagram in Fig. 1 behaves as a traditional PWM modulator [29].

III. Discrete-Time Click Modulator

Given a real, bandlimited, discrete-time signal $x[n]$, with discrete-time Fourier transform $X(e^{j\omega})$ that does not vanish over the interval $[-\omega_H, -\omega_L] \cup [\omega_L, \omega_H]$, with $0 < \omega_L < \omega_H < \pi$, let $\hat{x}[n]$ be its Hilbert transform. Therefore, $x_A[n] = x[n] + j\hat{x}[n]$ is an analytic signal whose spectrum $X_A(e^{j\omega})$ does not vanish within the interval $[\omega_L, \omega_H]$.

It may be tempting to define the discrete-time AEM as $z[n] = e^{-jx_A[n]}$. However, its frequency behaviour is quite different from its continuous-time counterpart due to the 2π-periodicity of the spectrum of discrete-time signals. To derive the spectrum of $z[n]$ it is again useful to express the exponential function as a power series

$$\begin{aligned} z[n] &= e^{-jx_A[n]} \\ &= \sum_{\ell=0}^{\infty} \frac{1}{\ell!} (-jx_A[n])^\ell \\ &= 1 + z_1[n] + \frac{1}{2!} z_2[n] + \frac{1}{3!} z_3[n] + \cdots \end{aligned} \tag{6}$$

where $z_\ell[n] = (-jx_A[n])^\ell$, and $z_0[n] \equiv 1$. The spectrum $Z(e^{j\omega})$ of $z[n]$ is given by:

$$Z(e^{j\omega}) = \sum_{\ell=0}^{\infty} \frac{1}{\ell!} Z_\ell(e^{j\omega}).$$

Applying the modulation or windowing theorem of the discrete-time Fourier transform ([47], pp. 61–62), the spectrum of the ℓ-th term in (6) is given by the $\ell - 1$ times convolution of the spectrum $Z_1(e^{j\omega})$ of $z_1[n]$:

$$\begin{aligned} Z_\ell(e^{j\omega}) &= Z_1(e^{j\omega}) \circledast \cdots \circledast Z_1(e^{j\omega}) \\ &= Z_{\ell-1}(e^{j\omega}) \circledast Z_1(e^{j\omega}) \end{aligned}$$

where "$\circledast$" denotes periodic convolution,

$$Z_\ell(e^{j\omega}) = \frac{1}{2\pi} \int_0^{2\pi} Z_{\ell-1}(e^{j\nu}) Z_1\left(e^{j(\omega-\nu)}\right) d\nu.$$

This equation reveals that the support of the spectrum $Z_\ell(e^{j\omega})$ of $z_\ell[n]$ is $[\ell\omega_L, \ell\omega_H]$, but due to the periodic nature of the spectrum of discrete-time signals some distortion may occur whenever $\ell\omega_L > 2\pi$ or $\ell\omega_H > 2\pi$. This situation is illustrated in Fig. 4 that shows the module of $Z_1(e^{j\omega})$, $Z_2(e^{j\omega})$ and $Z_3(e^{j\omega})$, which are the spectra of $z_1[n] = -jx_A[n]$, $z_2[n] = (-jx_A[n])^2$ and $z_3[n] = (-jx_A[n])^3$ in (6), respectively. Even though the spectrum of $z_1[n]$ is contained in $[\omega_L, \omega_H]$, with $0 < \omega_L < \omega_H < \pi$, some components of the spectrum of $z_2[n] = (-jx_A[n])^2$ may appear at frequencies higher than π. When computing the spectrum $Z_3(e^{j\omega})$ of $z_3[n] = (-jx_A[n])^3$, it results that $3\omega_H > 2\pi$, and therefore the part of the spectrum contained in the interval $[2\pi, 3\omega_H]$ is replicated every 2π. In particular, an alias appears within the interval $[0, \tilde{\omega}_H]$, where $\tilde{\omega}_H = 3\omega_H - 2\pi$. Also, due to the expansion of the spectrum the replicas overlap themselves, as indicated in the bottom panel of Fig. 4. This aliased component is responsible for distortion, and has to be removed if a distortion-free operation is desired. The case of the spectrum $Z_\ell(e^{j\omega})$ of higher order terms $z_\ell[n] = (-jx_A[n])^\ell$ in (6) is even worse, because it can result in multiple overlaps, spectral inversion, etc. However, although the ℓ-th therm may have a more complicated spectrum, its amplitude is scaled by $1/\ell!$ and therefore its deleterious effects on the final result of (6) are somewhat attenuated.

To overcome this problem, previous works use an interpolated version $x_{iA}[n]$ of the analytic signal $x_A[n]$ before applying (6) [30]–[36]. Interpolation by a factor M reduces the bandwidth of $x_{iA}[n]$ to the interval $[\omega_L/M, \omega_H/M]$, and therefore the number of terms in (6) that can be added without overlapping is increased. In other words, the exponential function is *approximated* by

$$z_i[n] = \sum_{\ell=0}^{L_i} \frac{1}{\ell!} z_\ell[n] \tag{7}$$

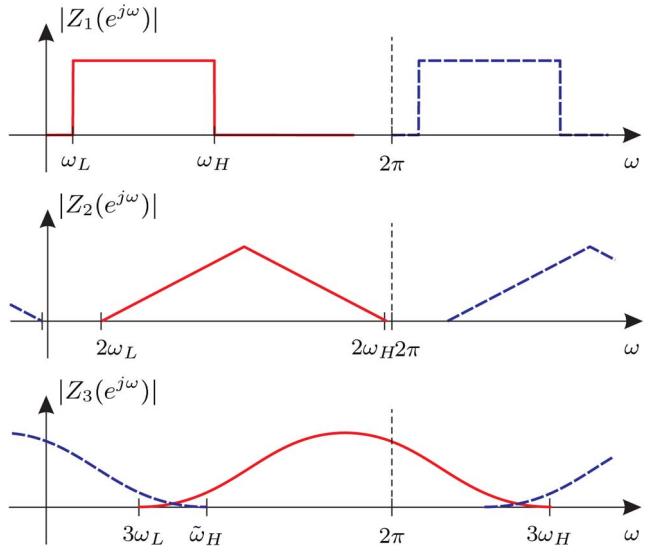

Fig. 4. Spectrum of the signals $x_A[n]$, $(x_A[n])^2$ and $(x_A[n])^3$.

where L_i is chosen so that $L_i\omega_H/M < 2\pi$, i.e., $L_i = \lfloor 2\pi M/\omega_H \rfloor$, with $\lfloor x \rfloor$ the floor function which is the largest integer not greater than x.

There is a trade-off between the interpolator order M and the approximation error; the higher the order M of the interpolator, the higher the number of terms L_i that can be used in (7) to approximate (6) with no aliasing, and it is expected that a lower approximation error may result. However, even (6) does not replicates the behaviour of the continuous AEM-LPF combination that is the key of the click modulator. Since $z_f[n]$ is bandlimited, it would be possible to avoid the aliasing problem if AEM and filtering are performed in a single processing block, as follows.

A. Simultaneous AEM and Filtering

To avoid the inconveniences described in the previous section, and to resemble the behaviour of the continuous-time click modulator, the filtered version of (6) is defined as:

$$\begin{aligned} z_f[n] &= 1 + \left[\sum_{\ell=1}^{\infty} \frac{1}{\ell!} \left(-jx_A[n] * h_H[n]\right)^\ell\right] * h_H[n] \\ &= 1 + \sum_{\ell=1}^{\infty} \frac{1}{\ell!} \left(-jx_A[n] * h_H[n]\right)^\ell * h_H[n] \\ &= 1 + \tilde{z}_1[n] + \frac{1}{2!}\tilde{z}_2[n] + \frac{1}{3!}\tilde{z}_3[n] + \cdots \end{aligned} \tag{8}$$

where $h_H[n]$ is the impulse response of the analytic, periodic bandpass filter defined in one period $0 \leqslant \omega < 2\pi$ as

$$H_H(e^{j\omega}) = \begin{cases} 1 & \text{if } \omega_L \leqslant \omega \leqslant \omega_U < \pi \\ 0 & \text{otherwise} \end{cases}$$

and

$$\begin{aligned}\tilde{z}_1[n] &= -jx_A[n] * h_H[n] * h_H[n] \\ &= -jx_A[n] * h_H[n] \\ \tilde{z}_2[n] &= (-jx_A[n] * h_H[n])^2 * h_H[n] \\ &= \tilde{z}_1^2[n] * h_H[n] \\ &= (\tilde{z}_1[n]\tilde{z}_1[n]) * h_H[n] \\ &\vdots \\ \tilde{z}_\ell[n] &= (-jx_A[n] * h_H[n])^\ell * h_H[n] \\ &= \tilde{z}_1^\ell * h_H[n] \\ &= \left(\tilde{z}_1^{\ell-1}[n]\tilde{z}_1[n]\right) * h_H[n].\end{aligned}$$

The spectrum of each of the terms in (8) is given by

$$\begin{aligned}\tilde{Z}_1(e^{j\omega}) &= Z_1(e^{j\omega})H_H(e^{j\omega}) \\ \tilde{Z}_2(e^{j\omega}) &= \left[\tilde{Z}_1(e^{j\omega}) \circledast \tilde{Z}_1(e^{j\omega})\right] H_H(e^{j\omega}) \\ &\vdots \\ \tilde{Z}_\ell(e^{j\omega}) &= \left[\tilde{Z}_1(e^{j\omega}) \circledast \cdots \circledast \tilde{Z}_1(e^{j\omega})\right] H_H(e^{j\omega}) \\ &= \left[\tilde{Z}_{\ell-1}(e^{j\omega}) \circledast \tilde{Z}_1(e^{j\omega})\right] H_H(e^{j\omega}).\end{aligned}$$

Using these auxiliary sequences, the spectrum $Z_f(e^{j\omega})$ of the bandlimited signal $z_f[n]$ can be written as:

$$Z_f(e^{j\omega}) = \delta(\omega) + \sum_{\ell=1}^{\infty} \frac{1}{\ell!} \tilde{Z}_\ell(e^{j\omega}).$$

The terms $\tilde{Z}_\ell(e^{j\omega})$ are different from zero for ω within the interval $[\ell\omega_L, \omega_U]$. The terms for which $\ell\omega_L > \omega_U$ do not contribute to the result. The above equation can be written as a finite sum

$$Z_f(e^{j\omega}) = \delta(\omega) + \sum_{\ell=1}^{L_\omega} \frac{1}{\ell!} \tilde{Z}_\ell(e^{j\omega}), \tag{9}$$

where $L_\omega = \lceil \omega_U/\omega_L \rceil$. The frequency components of each term in (9) are in the band $[\ell\omega_L, \omega_U]$, i.e., the sequences $\tilde{z}_\ell[n]$ computed recursively are already filtered and alias free. The value ω_U defines the so called baseband, and states that every frequency component below this value will be represented without distortion by the discrete-time click modulator. It is worth mentioning that (9) is the discrete-time equivalent of the CT-AEMF because no approximation has been performed. For this reason, it will be referred to as DT-AEMF.

The real signal $s[n]$ is derived from $z_f[n]$ as in the continuous-time case, i.e.,

$$s[n] = \mathrm{Re}\left\{\overline{z_f}[n]e^{j\omega_c n}\right\}$$

where $\omega_c = 2\pi f_c/f_s$. The square wave $q(t)$ is built using the zero-crossings of $s[n]$ and the carrier $x_c[n] = \sin(w_c n)$. The carrier frequency must be selected so that $\omega_c > \omega_U$.

B. Finite-Length Sequences

The method for computing the DT-AEMF has to be modified to deal with finite-length input sequences. Let $x[n]$ to be a N-point input sequence. If $x_A[n]$ is an analytic signal derived from $x[n]$ (see Appendix) the second half of its DFT $X_A[k]$ is zero, i.e.,

$$X_A[k] = 0, k = \begin{cases} N/2, \ldots, N-1, & \text{if } N \text{ is even} \\ (N-1)/2, \ldots, N-1, & \text{if } N \text{ is odd} \end{cases}$$

where the index associated with the lowest and highest frequency components is $N_L = \lfloor N\omega_L/(2\pi) \rfloor$ and $N_H = \lfloor N\omega_H/(2\pi) \rfloor$, respectively. The frequency behaviour of the AEM is analyzed using the power series of the exponential function given by (6). The spectrum $Z[k]$ of $z[n]$ is given by

$$Z[k] = \sum_{\ell=0}^{\infty} \frac{1}{\ell!} Z_\ell[k].$$

The DFT $Z_\ell[k]$ of the ℓ-th term can be written as (see the Appendix)

$$\begin{aligned}Z_\ell[k] &= \frac{1}{N^{\ell-1}} \left(Z_1[k] \circledN \cdots \circledN Z_1[k]\right) \\ &= \frac{1}{N} Z_{\ell-1}[k] \circledN Z_1[k]\end{aligned}$$

where $\circledN$ denotes N-point circular convolution,

$$Z_\ell[k] = \frac{1}{N} \sum_{m=0}^{N-1} Z_{\ell-1}[m] Z_1\left[((k-m))_N\right].$$

Each time a new product (convolution) is computed, the result must be scaled down by the factor $1/N$. This additional computation can be avoided if the first term is normalized by $1/N$.

As for the case for periodic convolution, this equation states that the DFT $Z_\ell[k]$ of $z_\ell[n]$ is different from zero for $k \in [\ell N_L, \ell N_H]$. However, distortion will appear whenever $\ell N_H > N$ due to the periodic nature of circular convolution. To avoid this effect, the DT-AEMF given by (8) is used. The DFT of the analytic filter $h_H[n]$ is defined by:

$$H_H[k] = \begin{cases} 1 & \text{if } N_L \leqslant k \leqslant N_U \\ 0 & \text{otherwise} \end{cases}$$

with $N_U = \lfloor N\omega_U/(2\pi) \rfloor < N/2$. The DFT of the terms in (8) is given by:

$$\begin{aligned}\tilde{Z}_1[k] &= Z_1[k]H_H[k] \\ \tilde{Z}_2[k] &= \left[\tilde{Z}_1[k] \circledN \tilde{Z}_1[k]\right] H_H[k] \\ &\vdots \\ \tilde{Z}_\ell[k] &= \left[\tilde{Z}_1[k] \circledN \cdots \circledN \tilde{Z}_1[k]\right] H_H[k] \\ &= \left[\tilde{Z}_{\ell-1}[k] \circledN \tilde{Z}_1[k]\right] H_H[k].\end{aligned} \tag{10}$$

The circular convolution results in no aliasing because the length of the sequences is lower than $N/2$. The DFT of the filtered signal $z_f[n]$ is

$$Z_f[k] = \delta[k] + \sum_{\ell=1}^{\infty} \frac{1}{\ell!} \tilde{Z}_\ell[k].$$

The terms $\tilde{Z}_\ell[k]$ are different from zero for $k \in [\ell N_L, N_U]$. The terms for which $\ell N_L > N_U$ do not contribute to the result. The above equation can be rewritten as:

$$Z_f[k] = \delta[k] + \sum_{\ell=1}^{L_U} \frac{1}{\ell!} \tilde{Z}_\ell[k], \tag{11}$$

where $L_U = \lceil N_U/N_L \rceil$. This expression reveals that an exact equivalent of the CT-AEMF behaviour can be obtained by a finite number of filtering and power operations in discrete-time.

In certain applications, L_U (although finite) can be large enough. This may be the case, for example, when $x[n]$ is a large sequence (N is large), $\omega_L = 2\pi/N$ ($N_L = 1$) and ω_U is set to its maximum allowed value, $\omega_U = \pi$, which results in $L_U = N/2$, a very large number. Therefore, sometimes it is desirable to obtain an approximation to $z_f[n]$ using fewer terms in (11). This is possible because the contribution of the successive terms in (11) decreases with $1/\ell!$. If the approximated signal is noted $z_L[n]$, its DFT is given by

$$Z_L[k] = \delta[k] + \sum_{\ell=1}^{L} \frac{1}{\ell!} \tilde{Z}_\ell[k]. \tag{12}$$

Experimentally, it has been found that the relationship between L and the resulting maximum Signal-to-Noise Ratio (SNR) in the baseband is given by:

$$\text{SNR [dB]} \approx 20 \log(L!) \tag{13}$$

C. Sampling Rate of the Input Signal

The sampling frequency defines the Nyquist limit, i.e., the maximum frequency value that can be represented and recovered without aliasing. For the digital click modulator, it would be desirable to define the guard band beyond $f_s/2$, i.e., $N_U > N/2$. A solution would be to sample the input signal at a higher rate to increase the system's bandwidth; thus requiring a change in the sampling frequency. However, the only effect in the spectrum is the addition of zeros for the higher frequencies. An alternative is to add zeros to the spectrum $X_A[k]$ of the analytic signal $x_A[n]$ from $N/2$ up to the desired index N_{DF} associated with the frequency point ω_{DF}. The subscript DF stands for *distortion free* and means that the frequencies in the band $[0, \omega_{DF}]$ will be modulated with no distortion by the digital click modulator. It is worth noting that the effect of the zero-padding over the signal $X_A[k]$ moves the Nyquist point from $f_{s_1}/2$ to $f_{s_2}/2$, being the quotient given by:

$$\frac{f_{s_2}}{f_{s_1}} = 2\frac{N_{DF}}{N}.$$

To avoid aliasing in the computation of $\tilde{Z}_\ell[k]$, the length of the circular convolution in (10) must be set to $M = 2N_{DF} - 1$. The advantage of using this technique is that the guard band and hence the switching frequency associated with click modulation is kept independent of the sampling frequency of the modulating signal.

D. Zero-Crossing Detection

Given a continuous-time signal that is represented from its samples by the sequence $s[n]$, its zero-crossings can be found when the sign of $s[n]$ changes between two consecutive time indexes.

In previous work, the zero-crossings were computed using a 3rd order polynomial built with 4 samples around a sign change [31]. Clearly, the detection improves as the sampling frequency increases. However, the main advantage of the proposed method for computing the DT-AEMF, is that the sampling frequency does not need to be increased. An alternative method for zero-crossing computation is introduced here.

The signal $s[n]$ can be thought as the sampled version of a continuous-time signal $s(t)$:

$$s(t) = \sum_{k=-R}^{R} S[k] e^{j\frac{2\pi}{T}kt}$$

where $S[k]$ is the DFT of $s[n]$ and $R = \lceil N f_c/f_s \rceil$ is the index associated with the carrier frequency. The zeros of $s(t)$ occur at

$$s(t) = \sum_{k=-R}^{R} S[k]\sigma^k = 0$$

with $\sigma = e^{j(2\pi/T)t}$. That is, $s(t)$ is a polynomial function of the variable σ. The polynomial can be written in terms of $Z_f[k]$, the DFT of $z_f[n]$:

$$P(\sigma) = \sum_{k=0}^{R} Z_f[k]\sigma^k + \sum_{k=1}^{R} \overline{Z_f}[R-k]\sigma^{R+k}. \tag{14}$$

The zeros of $P(\sigma)$ are complex and are all located in the unit circle. To map those zeros to the real axis, the inverse transformation must be applied over the variable σ. Notice that the phase of σ is $2\pi t_k/T$, where t_k is the zero and T the period of the signal $x(t)$. In terms of N and T_s, $T = NT_s$ and the value t_k is given by

$$t_k = \frac{\arg(\sigma) N T_s}{2\pi}. \tag{15}$$

The zeros computed using $P(\sigma)$ are exact unlike those obtained using the interpolation of the samples.

The binary signal $q(t)$ is obtained using (15) and the zeros of the carrier. Because the carrier is a sinusoidal waveform of known frequency, its zero-crossings do not need to be computed as they occur at:

$$t = \frac{k}{2f_c}, \text{ with } k = 0, 1, \ldots$$

This method for calculating the zero-crossings has proven to be useful when computing the off-line click modulator. The main

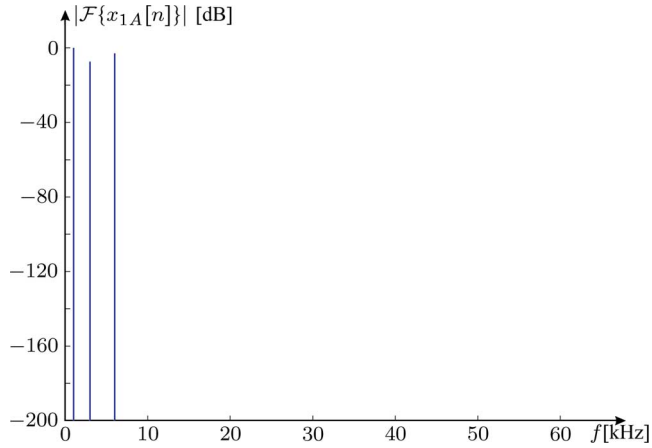

Fig. 5. Spectrum of the signal $x_{1A}[n]$.

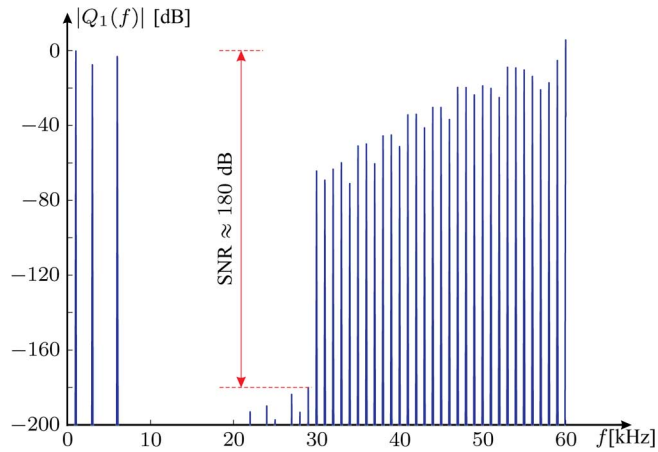

Fig. 6. Spectrum of the click-modulated signal $q_1(t)$.

problem is that the order of the polynomial $P(\sigma)$ used to compute the zeros tends to be high. This is due to the fact that the carrier frequency, which fixes R, depends on the selected guard band. If the distortion-free band is augmented, R would increase accordingly. A more efficient way of computing these zeros is currently under research.

IV. Experimental Results

An off-line version of the discrete-time click modulator was implemented. Two different scenarios were explored: (a) a multi tone signal comprised of three sine waves and (b) a bandpass-like signal. The objectives are to compare the performances of digital click modulation and Natural PWM, and to emphasize the real potential of digital click modulation.

The sampling frequency is $f_s = 60$ kHz and the carrier frequency is $f_c = 30$ kHz, which results on $q(t)$ switching at 60 kHz. The number of terms for implementing the DT-AEMF is $L = 12$, which using (13) results in $\mathrm{SNR} \approx 180$ dB. The baseband is defined between 0 and 30 kHz.

The signal $q(t)$ is a square wave with infinite harmonic components. Direct computation of its spectrum using the FFT would result in an important amount of aliasing. To overcome this problem the spectrum is obtained using the Fourier-by-Jumps method [48], [49], which allows the computation of the coefficients of the Fourier series of periodic, discontinuous signals.

A. Multi Tone Signal

The input is the multi tone signal

$$x_1(t) = 0.7\cos(2\pi 1000t) + 0.3\cos(2\pi 3000t) + 0.5\cos(2\pi 6000t).$$

The discrete-time sequence is $x_1[n] = x_1(t)|_{t=n/f_s}$, where $0 \leqslant n \leqslant N-1$. The length $N = 60000/1000 = 60$ represents only one period of the input signal. The spectrum of the analytic signal $x_{1A}[n]$ derived from $x_1[n]$ is shown in Fig. 5.

The DFT $Z_L[k]$ of the DT-AEMF output $z_L[n]$ is computed using (12) and the zero-crossings of $s(t)$ derived from the polynomial $P(\sigma)$ using (15). The square wave is then built using these values and the zero-crossings of the carrier.

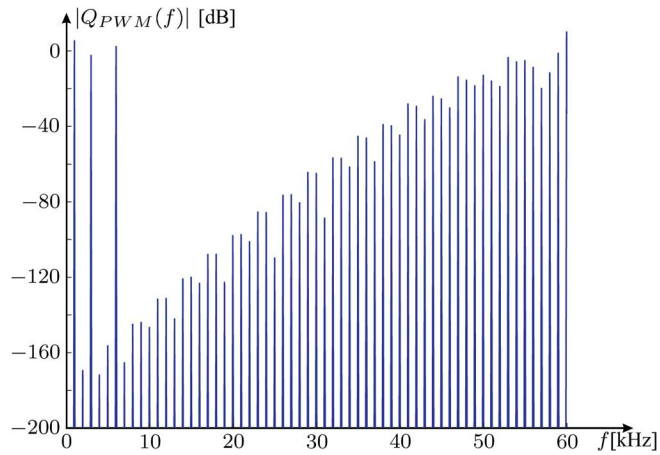

Fig. 7. Spectrum of the NPWM-modulated signal.

The spectrum of the resulting discrete-time click-modulated signal $q_1(t)$ is shown in Fig. 6, where it can be seen that the baseband information is separated from the high frequency harmonics. It is also verified that the maximum $\mathrm{SNR} \approx 180$ dB coincides with the predicted value for $L = 12$.

To prove the potential of the discrete-time click modulator, a comparison with NPWM was performed. The NPWM signal was obtained using symbolic mathematical manipulation to minimize numerical errors. Fig. 7 shows the spectrum that results from applying NPWM to the input signal $x_1(t)$. It can be seen that the continuous-time version of PWM performs well but it is impossible to get a distortion-free baseband. It is worth noting that uniform PWM would perform even worse. On the other hand, the proposed discrete-time click-modulator keeps the baseband free of distortion, even when sampling the input signal at the Nyquist limit.

B. Bandpass Signal

To test the discrete-time click modulator on a more realistic scenario, a bandpass signal $x_2[n]$ is used. The signal is speci-

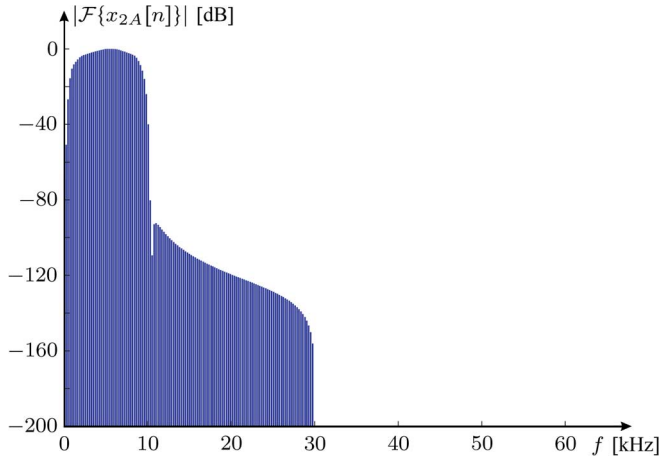

Fig. 8. Spectrum of the analytic signal $x_{2A}[n]$.

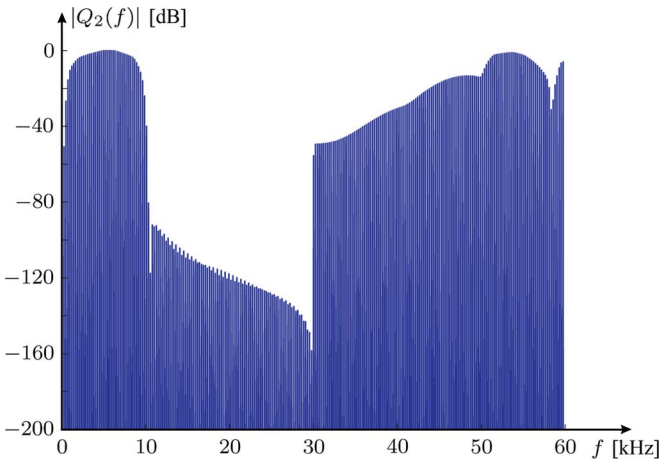

Fig. 9. Spectrum of the click-modulated signal $q_2(t)$.

fied by means of the frequency-sampling realization method, in which the parameters that characterize the signal are the values of the desired frequency response instead of the impulse response [50]. The length of the resulting signal $x_2[n]$ is $N = 256$ points, the sampling frequency $f_s = 60$ kHz and its spectrum is contained within the range 0 kHz and 30 kHz. The switching rate of the square wave $q_2(t)$ is 60 kHz. The spectrum of its analytic version $x_{2A}[n]$ is shown in Fig. 8. As in the example for the multi tone signal, the DFT $Z_L[k]$ of $z_L[n]$ is obtained from $X_{2A}[k]$ using (12) and the zero-crossings of $s(t)$ are derived from the polynomial $P(\sigma)$, mapping its zeros to the real axis with (15). The spectrum of the resulting digitally click-modulated signal $q_2(t)$ is shown in Fig. 9. It is verified that the baseband information is separated from the high frequency harmonics, starting at $f = 30$ kHz.

V. Conclusions

The first alias-free discrete-time click modulator was developed in this paper. The modulation algorithm is based on implementing the discrete-time AEM-LPF pair in one processing block, eliminating aliasing and the necessity of interpolating the input signal. DT-AEMF is carried out using circular convolution, which allows for direct/inverse FFT approach reducing the required computational power.

A detailed mathematical description was presented as well as practical simulation results. It was demonstrated that only a finite number of terms are needed to compute the DT-AEMF for bandpass signals. The number of terms can be limited in practice, without redesigning the filter. Additionally, an empirical formula was given for choosing the number of terms L to cope with a desired maximum SNR.

Zero-crossing detection is implemented using spectral information. This allows to obtain the exact switching times of the modulated signal.

In the experiments, the discrete-time click modulator behaves as expected, because baseband distortion was suppressed even using low switching-rates.

To prove the usefulness of the discrete-time click modulator, a comparison with NPWM was performed. It was shown that even the ideal continuous-time version of PWM introduces baseband distortion, while the proposed implementation of the discrete-time click modulator keeps the baseband information separated from the high frequency harmonics.

Although only simulation results are provided, a table containing the values of the zero-crossings could be used to synthesize a signal using a standard PWM module. This would allow the generation of high fidelity, low switching rates, and low distortion signals using an inexpensive hardware implementation.

Appendix

Analytic Finite-Length Sequences

To obtain the analytic signal $x_A[n]$ from the real signal $x[n]$ the following method is used [51]:

- compute the N-point DFT $X[k]$ of the signal $x[n]$.
- define the spectrum $X_i[k] = 2X[k]$ for $k \in [1, (N/2) - 1]$ and $X_i[k] = X[k]$ for $k = 0$ and $k = N/2$.
- make zero the negative part of the spectrum $X_i[k]$, that is $X_i[k] = 0$ for $k \in [(N/2) + 1, N - 1]$.
- compute the inverse DFT of $X_i[k]$ to get the signal $x_A[n]$.

Applying the previous steps the analytic signal $x_A[n]$ is derived. The real part of $x_A[n]$ is $x[n]$. The imaginary part of $x_A[n]$ is the Hilbert Transform of $x[n]$.

Modulation or Windowing Theorem for Finite-Length Sequences

Given the N-point sequence $x_1[n]$, the DFT $X_2[k]$ of the product $x_2[n] = x_1[n]x_1[n]$ is given by ([47], pp. 659):

$$X_2[k] = \frac{1}{N} X_1[k] \textcircled{N} X_1[k]$$

where $\textcircled{N}$ denotes N-point circular convolution. The spectrum $X_\ell[k]$ of the ℓ-th power of $x_1[n]$ is obtained convolving $\ell - 1$ times $X_1[k]$, i.e.,

$$\begin{aligned} X_\ell[k] &= \frac{1}{N}\frac{1}{N} \cdots \frac{1}{N} X_1[k] \textcircled{N} \cdots \textcircled{N} X_1[k] \\ &= \frac{1}{N^{\ell-1}} \left(X_1[k] \textcircled{N} \cdots \textcircled{N} X_1[k] \right). \end{aligned}$$

References

[1] Z. Song and D. V. Sarwate, "The frequency spectrum of pulse modulated signals," *Signal Process.*, vol. 83, pp. 2227–2258, Jul. 2003.

[2] D. M. Divan, "Optimum PWM waveform synthesis—A filtering approach," *IEEE Trans. Ind. Appl.*, vol. IA-21, no. 5, pp. 1199–1205, Sep./Oct. 1985.

[3] M. O. J. Hawksford, "Dynamic model-based linearization of quantized pulse-width modulation for applications in digital-to-analog conversion and digital power amplifier systems," *J. Audio Eng. Soc.*, vol. 40, no. 4, pp. 235–252, Apr. 1992.

[4] M. Yang and J. H. Oh, "Adaptive predistortion filter for linearization of digital PWM power amplifier using neural networks," in *Proc. 113th AES Convention*, Los Angeles, CA, Oct. 2002.

[5] P. Midya, B. Roeckner, and S. Bergstedt, "Digital correction of PWM switching amplifiers," *IEEE Power Electron. Lett.*, vol. 2, no. 2, pp. 68–72, Jun. 2004.

[6] G. Luckjiff and I. Dobson, "Hexagonal $\Sigma\Delta$ modulators in power electronics," *IEEE Trans. Power Electron.*, vol. 20, no. 5, pp. 1075–1083, Sep. 2005.

[7] P. Midya, B. Roeckner, and T. Paulo, "High performance digital feedback for PWM digital audio amplifiers," in *Proc. 121st AES Convention*, San Francisco, CA, Oct. 2006, Paper 6862.

[8] S. Saponara, L. Fanucci, and P. Terreni, "Oversampled and noise-shaped pulse-width modulator for high-fidelity digital audio amplifier," in *Proc. 13th IEEE Int. Conf. Electronics, Circuits Systems (ICECS)*, Nice, France, Dec. 2006, pp. 830–833.

[9] P. Midya, B. Roeckner, and T. Paulo, "Recursive natural sampling for digital PWM," in *Proc. 123rd AES Convention*, New York, Oct. 2007, Paper no. 7228.

[10] L. Peng, Y. Kang, X. Pei, and J. Chen, "A novel PWM technique in digital control," *IEEE Trans. Ind. Electron.*, vol. 54, no. 1, pp. 338–346, Feb. 2007.

[11] S. C. Huerta, A. de Castro, O. Garcia, and J. A. Cobos, "FPGA-based digital pulsewidth modulator with time resolution under 2 ns," *IEEE Trans. Power Electron.*, vol. 23, no. 6, pp. 3135–3141, Nov. 2008.

[12] M. Norris, L. M. Platon, E. Alarcon, and D. Maksimovic, "Quantization noise shaping in digital PWM converters," in *Proc. IEEE Power Electronics Specialists Conf. (PESC)*, Rhodes, Greece, Jun. 2008, pp. 127–133.

[13] M. G. Batarseh, W. Al-Hoor, L. Huang, C. Iannello, and I. Batarseh, "Window-masked segmented digital clock manager-FPGA-based digital pulsewidth modulator technique," *IEEE Trans. Power Electron.*, vol. 24, no. 11, pp. 2649–2660, Nov. 2009.

[14] A. De Castro and E. Todorovich, "High resolution FPGA DPWM based on variable clock phase shifting," *IEEE Trans. Power Electron.*, vol. 25, no. 5, pp. 1115–1119, May 2010.

[15] H. Ihs and C. Dufaza, "Digital-input class-D audio amplifier," in *Proc. 128th AES Convention*, London, U.K., May 2010, Paper 8128.

[16] C. H. Yang, C. W. Mu, and C. H. Tsai, "Synthesizable wide range DPWM with all-digital PLL for digitally-controlled switching converter," in *Proc. IEEE Annual Conf. Industrial Electronics (IECON)*, Melbourne, Australia, Nov. 2011, pp. 1626–1630.

[17] G. M. Sung, C. P. Yu, T. W. Hung, and H. Y. Hsieh, "Mixed-mode chip implementation of digital space SVPWM with simplified-CPU and 12-bit 2.56 Ms/s switched-current delta-sigma ADC in motor drive," *IEEE Trans. Power Electron.*, vol. 27, no. 2, pp. 916–930, Feb. 2012.

[18] C. Buccella, C. Cecati, and H. Latafat, "Digital control of power converters—A survey," *IEEE Trans. Ind. Inf.*, vol. 8, no. 3, pp. 437–447, Aug. 2012.

[19] N. D. Patel and U. K. Madawala, "A bit-stream based PWM technique for variable frequency sinewave generation," in *Proc. 13th IEEE Power Electronics Motion Contr. Conf. (EPE-PEMC)*, Poznań, Poland, Sep. 2008, pp. 139–143.

[20] N. D. Patel and U. K. Madawala, "A bit-stream based scalar control of an induction motor," in *Proc. 34th IEEE Annual Conf. Industrial Electronics (IECON)*, Orlando, FL, Nov. 2008, pp. 1071–1076.

[21] N. D. Patel and U. K. Madawala, "A bit-stream-based PWM technique for sine-wave generation," *IEEE Trans. Ind. Electron.*, vol. 56, no. 7, pp. 2530–2539, Jul. 2009.

[22] J. Bradshaw, U. Madawala, and N. Patel, "Techniques for conditioning high-speed bit-stream signals for power electronic applications," in *Proc. 35th IEEE Ann. Conf. Industrial Electronics (IECON)*, Porto, Portugal, Nov. 2009, pp. 142–147.

[23] E. R. C. Da Silva, E. C. Dos Santos, Jr., and C. B. Jacobina, "Pulsewidth modulation strategies," *IEEE Ind. Electron. Mag.*, vol. 5, no. 2, pp. 37–45, Jun. 2011.

[24] C. A. Yeh and Y. S. Lai, "Digital pulsewidth modulation technique for a synchronous buck DC/DC converter to reduce switching frequency," *IEEE Trans. Ind. Electron.*, vol. 59, no. 1, pp. 550–561, Jan. 2012.

[25] Y. M. Chen, Y. C. Chen, and T. F. Wu, "Feedforward delta modulation for power converters," *IEEE Trans. Ind. Electron.*, vol. 57, no. 12, pp. 4126–4136, Dec. 2010.

[26] T. D. Nguyen, J. Hobraiche, N. Patin, G. Friedrich, and J. P. Vilain, "A direct digital technique implementation of general discontinuous pulse width modulation strategy," *IEEE Trans. Ind. Electron.*, vol. 58, no. 9, pp. 4445–4454, Sep. 2011.

[27] A. K. Rathore, J. Holtz, and T. Boller, "Synchronous optimal pulsewidth modulation for low-switching-frequency control of medium-voltage multilevel inverters," *IEEE Trans. Ind. Electron.*, vol. 57, no. 7, pp. 2374–2381, Jul. 2010.

[28] Y. Wang, Q. Gao, and X. Cai, "Mixed PWM for dead-time elimination and compensation in a grid-tied inverter," *IEEE Trans. Ind. Electron.*, vol. 58, no. 10, pp. 4797–4803, Oct. 2011.

[29] B. F. Logan, Jr., "Click modulation," *AT&T Bell Lab. Tech. J.*, vol. 63, no. 3, pp. 401–423, Mar. 1984.

[30] M. Streitenberger and H. Bresch, "First implementation of a class-D amplifier with separated baseband," in *Proc. 10th Int. Symp. Theoretical Electrical Eng.*, Magdeburg, Germany, Sep. 1999, pp. 157–163.

[31] L. Stefanazzi, E. Paolini, and A. Oliva, "Click modulation: An offline implementation," in *Proc. 51st Midwest Symp. Circuits Systems (MWSCAS)*, Knoxville, TN, Aug. 2008, pp. 946–949.

[32] M. Streitenberger, F. Felgenhauer, H. Bresch, and W. Mathis, "Zero position coding (ZePoC)—A generalised concept of pulse-length modulated signals and its application to class-D audio power amplfiers," in *Proc. 110th AES Convention*, Amsterdam, The Netherlands, May 2001, Paper no. 8218.

[33] M. Streitenberger, F. Felgenhauer, H. Bresch, and W. Mathis, "Zero-Pposition coding with separated baseband in low-power class-D audio amplifiers for mobile communications," in *Proc. 5th IEEE Int. Conf. Telecommunications in Modern Satellite, Cable and Broadcasting Service (TELSIKS)*, Niš, Yugoslavia, Sep. 2001, pp. 567–570.

[34] M. Streitenberger, F. Felgenhauer, H. Bresch, and W. Mathis, "Class-D audio amplifiers with separated baseband for low-power mobile applications," in *Proc. 1st IEEE Int. Conf. Circuits Syst. Commun. (ICCSC)*, St. Petersburg, Russia, Jun. 2002, pp. 186–189.

[35] M. Streitenberger and W. Mathis, "A novel coding topology for digital class-D audio power amplifiers with very low pulse-repetition rate," in *Proc. 28th European Solid-State Circuits Conf. (ESSCIRC)*, Firenze, Italy, Sep. 2002, pp. 515–518.

[36] K. P. Sozanski, "A digital click modulator for a class-D audio power amplifier," in *Proc. Signal Process. Algorithms, Architectures, Arrangements, and Applications (SPA)*, Poznan, Poland, Sep. 2009, pp. 121–126.

[37] A. R. Oliva, E. Paolini, and S. S. Ang, "A new audio file format for low-cost, high-fidelity, portable audio amplifiers," presented at the Texas Instrument Incorporated, Oct. 2005, white paper, SPRY076.

[38] E. Bedrosian, "The analytic signal representation of modulated waveforms," *Proc. IRE*, vol. 50, no. 10, pp. 2071–2076, Jul. 1962.

[39] H. B. Voelcker, "Toward a unified theory of modulation—Part I: Phase-envelope relationships," *Proc. IEEE*, vol. 54, no. 3, pp. 340–353, Mar. 1966.

[40] H. B. Voelcker, "Toward a unified theory of modulation—Part II: Zero manipulation," *Proc. IEEE*, vol. 54, no. 5, pp. 735–755, May 1966.

[41] B. F. Logan, Jr., "Information in the zero crossings of bandpass signals," *B. S. T. J.*, vol. 56, no. 4, pp. 487–510, Apr. 1977.

[42] B. F. Logan, Jr., "Theory of analytic modulation systems," *B. S. T. J.*, vol. 57, no. 3, pp. 491–576, Mar. 1978.

[43] B. F. Logan, Jr., "Signals designed for recovery after clipping—I. Localization of infinite products," *AT&T Bell Lab. Tech. J.*, vol. 63, no. 2, pp. 261–285, Feb. 1984.

[44] B. F. Logan, Jr., "Signals designed for recovery after clipping—II. Fourier transform theory of recovery," *AT&T Bell Lab. Tech. J.*, vol. 63, no. 2, pp. 287–306, Feb. 1984.

[45] B. F. Logan, Jr., "Signals designed for recovery after clipping—III: Generalizations," *AT&T Bell Lab. Tech. J.*, vol. 63, no. 3, pp. 379–399, Mar. 1984.

[46] R. N. Bracewell, *The Fourier Transform and Its Applications*, 3rd ed. , Singapore: McGraw-Hill, 1999.

[47] A. V. Oppenheim and R. W. Schafer, *Discrete-Time Signal Process.*, 3rd ed. Upper Saddle River, NJ: Prentice Hall, 2009.

[48] M. A. Slonim, "Harmonic analysis of periodic discontinuous functions (new method). Part I—Exponential functions," *Proc. IEEE*, vol. 67, no. 6, pp. 952–953, Jun. 1979.

[49] M. A. Slonim, "Harmonic analysis of periodic discontinuous functions (new method). Part II—Polynomial functions," *Proc. IEEE*, vol. 67, no. 6, pp. 953–954, Jun. 1979.

[50] J. G. Proakis and D. G. Manolakis, *Digital Signal Process.—Principles, Algorithms, and Applications*, 3rd ed. Upper Saddle River, NJ: Prentice Hall, 1996.
[51] R. G. Lyons, *Understanding Digital Signal Process.*, 2nd ed. Upper Saddle River, NJ: Prentice Hall, 2004.

Leandro Stefanazzi received the B.S. degree in electronic engineering and the M.S. degree in Control Systems from Universidad Nacional del Sur, Bahía Blanca, Argentina, in 2006 and 2008, respectively.

From June 2009 and up to November 2010, he joined the Electronics and Information Technology Laboratory of the French Atomic Energy Commission (CEA-LETI) as a Research Engineer in the areas of communications for 3GPP/LTE standards. He is currently a Ph.D. student of the Secretaría de Posgrado y Educación Continua at Universidad Nacional del Sur. His research interests are in the areas of digital signal processing and power electronics.

Alejandro R. Oliva received the B.S.E.E. degree from the Universidad Nacional del Sur, Bahía Blanca, Argentina, in 1987, and the M.S.E.E. and Ph.D. degrees in electrical engineering from the University of Arkansas at Fayetteville, Arkansas, in 1996 and 2004, respectively.

He is a Professor at the Electrical Engineering Department of the Universidad Nacional del Sur, Baha Blanca, Argentina, since 1999. Since 2005 he is a member of CONICET. He. He has published a book and more than 50 papers in journals and proceedings. His main research interests are Power electronics and Power management.

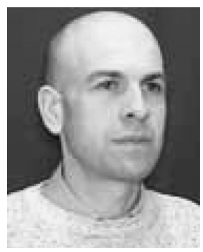

Eduardo E. Paolini is Professor at the Electrical Engineering Department of the Universidad Nacional del Sur, Bahía Blanca, Argentina, since 1998, and a member of Comisión de Investigaciones Científicas de la Provincia de Buenos Aires (CIC) since 2011.

His research interests are digital signal processing, and switched and nonlinear systems.